ORIGINAL PAPER

Dynamics of CO_2 fluxes and controlling environmental factors in sugarcane (C4)–wheat (C3) ecosystem of dry sub-humid region in India

N. R. Patel[1] · Shweta Pokhariyal[1] · Prakash Chauhan[1] · V. K. Dadhwal[2]

Abstract

In this study, CO_2 exchange over sugarcane and wheat growing season was quantified by continuous measurement of CO_2 fluxes using eddy covariance (EC) system from January 2014 to June 2015. We also elaborated on the response of CO_2 fluxes to environmental variables. The results show that the ecosystem has seasonal and diurnal dynamics of CO_2 with a distinctive U-shaped curve in both growing seasons with maximal CO_2 absorption reaching up to -8.94 g C m^{-2} day^{-1} and -6.08 g C m^{-2} day^{-1} over sugarcane and wheat crop, respectively. The ecosystem as a whole acted as a carbon sink during the active growing season while it exhibits a carbon source prior to sowing and post-harvesting of crops. The cumulative net ecosystem exchange (NEE), gross primary productivity (GPP), and ecosystem respiration (R_{eco}) were -923.04, 3316.65, and 2433.18 g C m^{-2} over the sugarcane growing season while the values were -192.30, 621.47, and 488.34 g C m^{-2} over the wheat growing season. The sesbania (green manure) appeared to be a carbon source once it is incorporated into soil. The response of day-time NEE to photosynthetically active radiation (PAR) under two vapor pressure deficit (VPD) sections (0–20 h Pa and 20–40 h Pa) seems more effective over sugarcane ($R^2 = 0.41$–0.61) as compared to the wheat crop ($R^2 = 0.25$–0.40). A decrease in net CO_2 uptake was observed under higher VPD conditions. Similarly, night-time NEE was exponentially related to temperature at different soil moisture conditions and showed higher response to optimum soil moisture conditions for sugarcane ($R^2 = 0.87$, $0.33 \leq$ SWC $<$ 0.42 m^3 m^{-3}) and wheat ($R^2 = 0.75$, $0.31 \leq$ SWC $<$ 0.37 m^3 m^{-3}) crop seasons. The response of daily averaged NEE to environmental variables through path analysis indicates that PAR was the dominant predictor with the direct path coefficient of -0.65 and -0.74 over sugarcane and wheat growing season, respectively. Satellite-based GPP products from Moderate Resolution Imaging Spectroradiometer (GPP$_{MOD}$) and Vegetation Photosynthetic model (GPP$_{VPM}$) were also compared with the GPP obtained from EC (GPP$_{EC}$) technique. The seasonal dynamics of GPP$_{EC}$ and GPP$_{VPM}$ agreed well with each other. This study covers the broad aspects ranging from micro-meteorology to remote sensing over C4-C3 cropping system

Keywords Sugarcane · Wheat · Eddy covariance technique · NEE · Path analysis

✉ N. R. Patel
   nrpatel@iirs.gov.in

   Shweta Pokhariyal
   shwetapokhariyal@iirs.gov.in

   Prakash Chauhan
   prakash@iirs.gov.in

   V. K. Dadhwal
   vkdadhwal@iist.ac.in

[1] Indian Institute of Remote Sensing, ISRO, Govt. of India, 4, Kalidas Road, Dehradun, Uttarakhand 248001, India

[2] Indian Institute of Space Science and Technology, Thiruvananthapuram, Kerala 695547, India

Introduction

Achieving climate-resilient agriculture to counteract the threat of global warming and make a positive impact on the sustainable development goal of "Zero Hunger" is a prime focus of the global scientific community. Monitoring of carbon budget and subsequently the sink and sources of CO_2 from terrestrial ecosystems plays a dominant role in mitigating climate change due to rising atmospheric CO_2. The quantification of the carbon budget of any ecosystem demands long-term monitoring of the biosphere–atmosphere exchange of scalars and energy in combination with governing eco-physiological variables (Baldocchi et al. 2001). Continuous and long-term monitoring of CO_2 fluxes from diverse ecosystems has thus become

critical in developing a mitigation strategy to reduce carbon emission and enhance carbon sequestration.

Substantial usage of the eddy covariance technique worldwide since the 1980s (e.g., AsiaFlux, EUROFLUX, AmeriFlux networks) proved its capability to measure and analyze the carbon sequestration potential in the terrestrial ecosystem. The phenomenal quality of this technique is to measure CO_2 and H_2O fluxes on varying spatial (ranging from a single crop field to an extensive forest landscape) and temporal scales (varying from half-hourly to yearly). Although a majority of previous studies were mainly focused over grassland and forest ecosystems (Joon Kim et al. 1992; Mielnick and Dugas 2000; Ansley et al. 2002; Kaul et al. 2009; Hernandez-Ramirez et al. 2011), the study on CO_2 exchange over agricultural ecosystem is gradually expanding. Scientists have executed a detailed analysis of intra- and inter-annual variations of CO_2 fluxes (Murayama et al. 2003; Aubinet et al. 2009; Glenn et al. 2010). Some have dealt with data processing (Soegaard et al. 2003; Saito et al. 2009) while others focused on the response of environmental variables on CO_2 fluxes in different crop sites (Suyker et al. 2004; Moureaux et al. 2008; Béziat et al. 2009; Ceschia et al. 2010). Besides this wide network to measure CO_2 and H_2O fluxes on varying spatial and temporal scales, poor representation of the Indian subcontinent for eddy covariance (EC) towers may lead to large uncertainty in quantifying the South Asian Carbon budget (Patra et al. 2013). The EC technique is a unique micrometeorological method with high sampling rate and short response time. It provides the continuous flux measurements over large area with detailed information on the short-term fluxes variation.

The establishment of EC flux-towers aimed at quantification of carbon exchanges over varied ecosystems in India was initiated with the inception of the National Carbon Project under the Geosphere-Biosphere Programme of Indian Space Research Organisation (Dadhwal et al., 2010; Jha et al. 2013; Patel et al. 2011; Watham et al. 2014). Later ecosystem flux research gained momentum to cover vast Indian landmass with large heterogeneity in land covers, climate regimes, and physiography (Chatterjee et al. 2018; Deb Burman et al. 2019). Previous studies in India were mainly focused over forest ecosystems (Jha et al. 2013; Watham et al. 2014; Sarma et al. 2018) and few over cropland preferably dominant cereal-based cropping system (Patel et al. 2011; Bhattacharyya et al. 2013; Deb Burman et al. 2020). These efforts seem meager to represent the vast landmass of cropland with diverse cropping systems in India. Furthermore, to the best of our knowledge, there is no carbon flux report addressed over the sugarcane (C4)-wheat (C3)-based cropping system. This cropping system having a combination of cash (sugarcane) and cereal (wheat) crop offers financial and food security of rural livelihood. Sugarcane possesses the capability of being most advantageous among agronomic crops

owing to its higher productivity and return on energy investment (Goldemberg et al. 2008; Waclawovsky et al. 2010), further catalyzing its propensity towards higher greenhouse gas reductions in comparison to other agronomic biofuels (de Vries et al. 2010; Davis et al. 2012).

India earmarked its topmost position in the sugarcane and wheat production, accounting for 22.82% and 12.05%, respectively, in the total world's production. These crops are dominantly manifested in a paddy-autumn sugarcane-ratoon-wheat–based system in the sub-tropical region of India. Further, the difference in photosynthetic pathways (C3 and C4) of these crops enhances the scope of comparative analysis of carbon sequestration potential of the sugarcane-wheat cropping system. Over the last two decades, substantial work being carried out across the world to elucidate variation in carbon and water fluxes over agroecosystems (Pearcy and Ehleringer 1984); (Baldocchi 1994; Li et al. 2006; Aubinet et al. 2009; Béziat et al. 2009). Owing to the non-intrusive nature of the EC technique, it has been widely utilized for carbon accounting of croplands comprising both C3 and C4 crops, for example, carbon balance over a C3 (wheat)-C4 (maize) cropping system (Yongqiang et al. 2002; Lei et al. 2011), C3 (wheat) crop (Patel et al. 2011; Wang et al. 2013; Saha et al. 2015; Chi et al. 2017), and C4 (sugarcane) crop (Teixeira et al. 2013; Cabral et al. 2013; Anderson et al. 2015). Keeping all the facts in mind, the comparative study over C4 (sugarcane) and C3 (wheat) crop rotation mainly practiced in the fertile region of Indo-Gangetic plains of India (Pathak et al. 2014) is the prime need in the context of the research program on climate change. The major objectives of this study are two-fold: (1) to quantify CO_2 fluxes and seasonal variation over the sugarcane-wheat cropping system with characteristic behavior of C4 and C3 photosynthetic pathways, (2) to assess the environmental control on net ecosystem exchange (NEE) of sugarcane and wheat crop in the sub-tropical climate of Upper Indo-Gangetic plains.

Material and methods

Site description

The study site was an extensive agricultural land located in southern direction, about 28 km far from Saharanpur district of Uttar Pradesh. This area can be characterized under a dry sub-humid, megathermal climate. The mean annual temperature is 23.4 °C, with a maximum (43.9 °C) and minimum (3.7 °C) temperature in June and January, respectively. The mean annual precipitation is 1204 mm, a large portion of which falls from July to September. The distinctive cropping system in the Saharanpur region consists of sugarcane, wheat, rice, and maize.

In the present study, we dealt with a ratooned sugarcane-wheat-sesbania cropping system, having a sugarcane crop from February 2014 to October 2014, wheat crop in winter from November 2014 to April 2015, and sesbania (*Sesbania rostrata*) from end April 2015 to June 2015. The soil in the region is coarse sandy loam, with mean bulk density of 1.55 g cm^{-3}.

Flux and micrometeorological measurement

Instruments for measuring eddy covariance and micro-climatic variables were installed on a tripod mast of measurement tower located at the study site (29° 52′ 19.139″ N and 077° 34′ 01.621″ E). CO_2 fluxes between the land surface and the atmosphere were measured from January 2014 to June 2015 using EC system installed at a height of 3.5 m above the ground surface. The EC system consists of the open-path gas analyzer (Li-7500, IRGA, Li-Cor., Lincoln, NE, USA) along with a 3D sonic anemometer (CSAT-3, Campbell Scientific). Measured data were sampled at a frequency of 10 Hz using a fast response data logger (Model CR1000, Campbell Scientific, USA). The vertical CO_2 flux density was obtained as the covariance between the CO_2 mixing ratio (c') and vertical fluctuations (w').

Apart from the flux measurements, the ancillary meteorological measurements during the whole study period were also recorded. The net radiation was measured using the net radiometer (CNR1, Kipp and Zonen) installed at 1.5 m above the ground surface. It is a four-component device with a pair of pyranometer and pyrgeometer, used to measure shortwave and longwave radiation, respectively. The ambient temperature and relative humidity was recorded using the temperature-humidity sensor (HMP-45, Vaisala, Inc., Finland). Soil temperature probes were inserted at the depth of 0.075 m and 0.15 m to measure soil temperature. Soil water content (SWC) was measured using CS616 soil moisture sensors placed at 0.05, 0.10, and 0.15 m depth. The soil heat flux component was measured using a HFP01 soil heat flux plate (Campbell Scientific Inc.) placed at the depth of 0.075 m.

The rainfall data was taken from the nearby meteorological station located at 29° 58′ N latitude and 77° 33′ E longitude. We also computed the water availability index (WAI) to examine the water availability in the study region (Wang and Li Xin 2020). It is the ratio of actual evapotranspiration and potential evapotranspiration (PET) and ranges from 0 to 1 representing well-watered to water-stressed conditions. The AET and PET were derived from EC measurements and by the Penman-Monteith equation (Allen et al. 1998), respectively.

Field LAI measurements

The ACCUPAR Model LP-80 (Decagon devices, Pullman, WA, USA), a battery-operated linear photosynthetically active radiation (PAR) ceptometer, was used to calculate leaf area index (LAI) non-destructively in real time in the field. The AccuPAR calculates the LAI based on the above- (P_a) and below-canopy PAR (P_b) measurements along with the parameters related to the position of the sun and the canopy architecture using transmission and scattering equation (Supplementary material) of Norman and Jarvis, 1975.

We measured P_a and P_b values above and below the crop canopy, respectively, to obtain LAI. P_a measurements were obtained by placing LP-80 above the canopy in an unshaded region. P_b was obtained as an average of the 5 individual readings taken in different probe direction parallel or perpendicular to the crop rows. Similarly, the measurements were taken randomly from the 3 points in the field and then averaged to obtain the LAI for that particular time.

Data analysis and processing

Raw data obtained from EC flux tower was further processed in the datalogger starter software (PC200W) to split the obtained dataset into half-hourly intervals. Subsequently, data were processed offline using Eddy Pro 6.2.0 Software (LI-COR, Lincoln, NE, USA). Obtained half-hourly EC data was rejected on the following criteria: (1) incomplete half-hourly dataset; (2) night-time dataset under stable conditions corresponding to u*< 0.1 ms^{-1} (Figure S1). Approximately 16.44% and 28.32% data was lost due to instrument malfunction, power failure, and the above specified criteria.

Gap-filling

EC system can rarely produce good quality data for whole year. Several reasons exist for the gaps, and it is required to fill the gaps for annual estimates (Anthoni et al. 2004). Gap-filling was done using the following techniques:

1. For small gaps (< 2 h), missing data was linearly interpolated (Aubinet et al. 1999).
2. For the gaps over 2 h, night-time and day-time fluxes were filled separately by establishing relationship between meteorological parameters, provided the corresponding meteorological parameters remain complete.

   Day-time gaps were filled by expressing a rectangular hyperbolic function (Michaelis-Menten equation) between the gross primary productivity (GPP) and PAR on a monthly basis (Falge et al. 2002).

$$F_{GPP,day} = \frac{\alpha * PAR * Pmax}{\alpha * PAR + Pmax} \quad (1)$$

where $F_{GPP,day}$ is day-time GPP, α represents initial slope of light use efficiency curve (μ mol μ mol^{-1} photons), and Pmax

is the maximum photosynthetic rate at light saturation (μ mol CO_2 m^{-2} s^{-1}). The model (Eq. 1) was fitted using Origin 9.0 software (Micro Cal Software Inc.).

Night-time missing data were filled by using a simple exponential relationship between net ecosystem exchange and air temperature under unstable condition (u* > 0.1 ms^{-1})

$$F_{\text{NEE,night}} = a \exp^{(b*\text{Ta})} \qquad (2)$$

where $F_{\text{NEE,night}}$ is net ecosystem exchange (NEE) during night-time, a and b are empirical constants, and Ta is the air temperature. Ecosystem respiration during day-time (Rd) was extrapolated from Eq. (2). The negative NEE values imply net CO_2 uptake by the vegetation while positive NEE values indicate net CO_2 release into the atmosphere by the vegetation.

Q_{10} was calculated according to the Van't Hoff equation:

$$Q_{10} = e^{10b} \qquad (3)$$

where Q_{10} is the temperature sensitivity of $F_{\text{NEE,night}}$ or night-time respiration (R_n) and b is the empirical constant which reflects the temperature sensitivity of R_n

Net ecosystem respiration (Rn) during night-time can be considered as a source of entire CO_2 flux due to absence of photosynthetic activity (Vote et al. 2015). Subsequently, net ecosystem respiration (R_{eco}) was the sum of Rn (net ecosystem respiration during night-time) and Rd (net ecosystem respiration during day-time).

$$R_{\text{eco}} = \text{Rn} + \text{Rd} \qquad (4)$$

Subsequently, NEE was partitioned into GPP and R_{eco} using (Eq. 5)

$$\text{GPP} = -\text{NEE} + R_{\text{eco}} \qquad (5)$$

where GPP denotes gross primary productivity (μ mol CO_2 m^{-2} s^{-1}), NEE is net ecosystem exchange (μ mol CO_2 m^{-2} s^{-1}), and R_{eco} is net ecosystem respiration (μ mol CO_2 m^{-2} s^{-1}).

In our study site, incomplete flux dataset was available for the months of January, February, March, November, and December of 2014. To represent the flux dataset on a yearly basis, we gap-filled the aforementioned months based on the available meteorological parameters. We applied the Michaelis-Menten equation and exponential temperature equation to fill day-time and night-time data, respectively.

Path analysis

Dependence of NEE on five primarily affecting environmental variables {PAR, Ta, vapor pressure deficit (VPD) and SWC, WAI} was evaluated using path analysis with EC data collected over sugarcane and wheat growing season. Path analysis is an extension of multiple regression which is a useful analysis tool when correlative information of relationship among variables is known in prior (Li 1981). Further, it acts as an appropriate tool, when the independent nature of predictor variables is not certain and is expected to depend on one another. Path analysis is effectively used in many ecological studies (Bassow and Bazzaz 1998; Xu and Qi 2001; Huxman et al. 2003; Zhuang et al. 2004; Saito et al. 2009).

In the present study, path analysis was done to partition the correlation coefficient into direct and indirect effect on variables. The direct effect is the standardized partial regression coefficient of the dependent variable y and independent variable i, which indicates the direct impact of i on y. The indirect effect indicates how the independent variables influence each other, which in turn affects the dependent variable.

$$r_{\text{yi}} = P_{1y}r_{1i} + P_{2y}r_{2i} \ldots\ldots + P_{ny}r_{ni} \ (i = 1, 2, 3 \ldots n) \qquad (6)$$

where r_{yi} represent the correlation coefficient between dependent variable y and independent variable i, P_{ny} is the direct effect of the independent variable n on dependent variable y, r_{ni} is the correlation between independent variables (i and n), and $P_{ny} \times r_{ni}$ is used to express the indirect path coefficient of i through n on y.

Satellite-based GPP products

In the present study, we utilized the available GPP products from January 2014 to June 2015. The GPP products include the GPP from Moderate Resolution Imaging Spectroradiometer (MODIS) dataset and Vegetation Photosynthesis Model (VPM) (Supplementary material 2.2) The MODIS GPP (GPP_{MOD}) obtained from the MODIS version 6 (MOD17A2H.006) is a cumulative 8-day composite with a 500-m spatial resolution. The GPP_{MOD} values were extracted on an 8-day basis from the study site using the Google Earth Engine platform (GEE).

GPP from the VPM model (GPP_{VPM}) was also utilized to compare with the observed GPP from the EC tower site (GPP_{EC}). The GPP_{VPM} product is available at 8-day temporal resolution with a moderate spatial resolution of 500 m over the entire globe from the years 2000 to 2016. The GPP_{VPM} product was downloaded from the US Department of Agriculture (https://data.nal.usda.gov/dataset/global-moderate-resolution-dataset-gross-primary-production-vegetation-2000%E2%80%932016). The obtained GPP products (GPP_{VPM} and GPP_{MOD}) available at an 8-day interval were then compared with the 8-day GPP_{EC}.

Results and discussion

Variation in meteorological variables

The variation in meteorological variables over the 2014–2015 growing season is shown in Fig. 1. The observed seasonal

Fig. 1 Variation of meteorological parameters at Saharanpur flux site (SFS) in 2014 (left) and 2015 (right). (a) Sum of photosynthetically active radiation (MJm^{-2} day^{-1}), (b) daily mean air temperature (°C), (c) mean day-time vapor pressure deficit (h Pa), (d) soil water content (m^3 m^{-3}) at a depth of 7.5 cm, (e) rainfall (mm), and (f) leaf area index. Bar indicates ±SD. Dashed line in middle of the graph represents bifurcation between the years 2014 and 2015
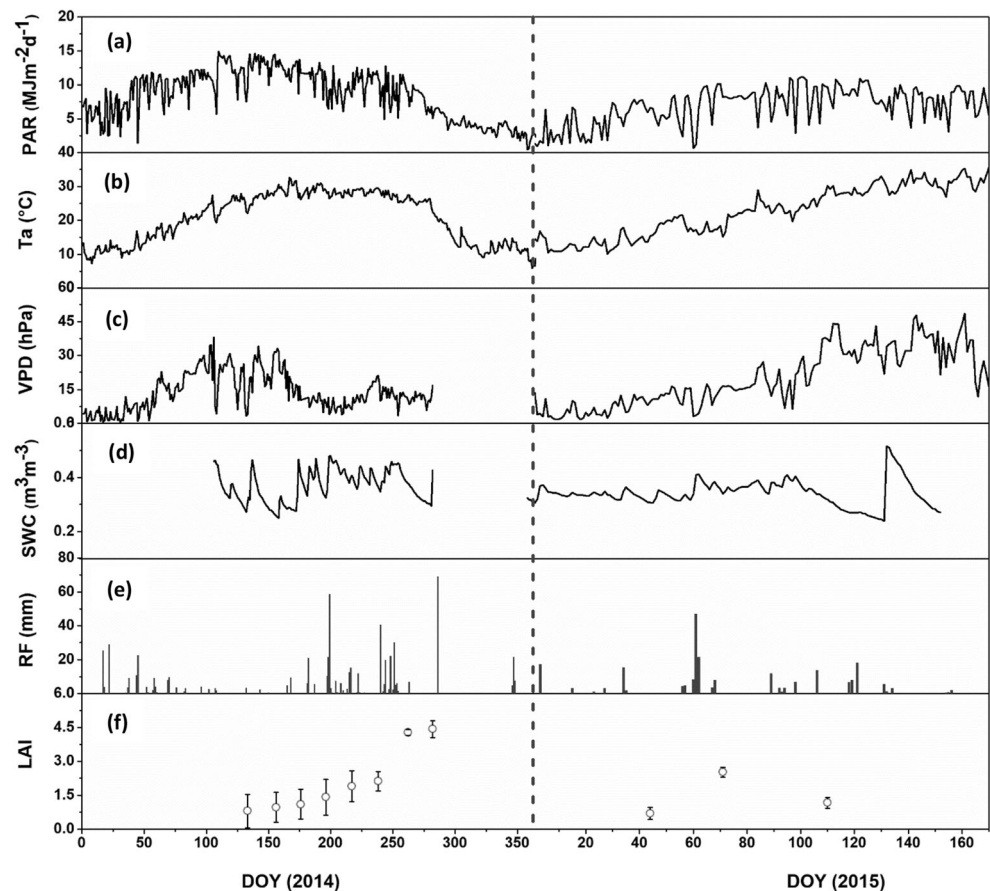
trend was almost similar for VPD and PAR. The average air temperature was 26.49 °C and 22.30 °C for 2014 and 2015 growing season, respectively. Daily average SWC (measured at 7.5 cm) varied significantly ranging from 0.25 to 0.47 m^3 m^{-3} and 0.23 to 0.51 m^3 m^{-3} for the years 2014 and 2015, respectively. The mean day-time VPD values range from 1.02 to 38.55 hPa and 1.64 to 48.60 hPa in the years 2014 and 2015, respectively.

The seasonal average of PAR during sugarcane (Feb 2014–October 2014), wheat (Dec 2014–April 2015), and sesbania (May 2015–June 2015) growing season was 9.97, 5.74, and 7.88 M J m^{-2} day^{-1}, respectively. The average seasonal air temperature was 30.03 °C, 19.54 °C, and 30.11 °C for sugarcane, wheat, and sesbania growing season, respectively. Volumetric soil water content (SWC) was higher during the sugarcane growth period as compared to that in wheat season, reaching its maximum in July (0.41 m^{3}m^{-3}). SWC in the wheat growing season varies from 0.37 m^{3}m^{-3} (March) to 0.32 m^{3}m^{-3} (February). The daily rainfall (RF) shows clear seasonal patterns, and was mainly distributed in the growing period. Considering the study period from January 2014 to June 2015, the annual rainfall shows large variation, ranging from 618.6 mm (Jan 2014 to Dec 2014) to 224.2 mm (Jan 2015–June 2015). RF is highest during June–August and reduced during the winter season.

The meteorological parameter assessed during sugarcane-wheat-sesbania growing season showed great variability which further provided an excellent opportunity to quantify the impact of climate variability on CO_2 exchange.

Diurnal dynamics of carbon dioxide fluxes

The mean of 30-min NEE has been represented through NEE fingerprint plot (Fig. 2A). The diel NEE variation revealed that the CO_2 absorption dominates the carbon release after around 8:00 hr. The blue colored portion in the fingerplot depict CO_2 uptake which peaks around 10:30 to 14:00 hrs. The 30-min NEE growing season ranged from −49.8 to 39.3 μ mol m^{-2} s^{-1} over the sugarcane growing season. NEE ranged from −22.63 to 20.75 μ mol m^{-2} s^{-1} during the wheat growing season. During the sesbania growing season, the NEE ranged from −13.41 to 16.40 μ mol m^{-2} s^{-1}, which later increased up to 31.81 μ mol m^{-2} s^{-1}, after its incorporation into the soil.

Figure 2B shows the monthly diurnal variation in NEE during the sugarcane and wheat growing seasons. It depicted that the ecosystem acted as a strong CO_2 sink during the active vegetative period and a CO_2 source during the senescence phase. Diurnal variation in winter months (December and January) was not quite remarkable, owing to bare soil, low temperature, and low PAR. During the main growing season

Fig. 2 (A) NEE fingerprint plot representing half-hourly NEE (μmol m^{-2} s^{-1}) during whole study period. The thick dashed line represents the start of the (a) sugarcane growing season, (b) fallow period, (c) wheat growing season, and (d) sesbania growing season. (B) Diurnal variation of net ecosystem CO_2 exchange (NEE) in different months of growing seasons of crops (a) sugarcane and (b) wheat
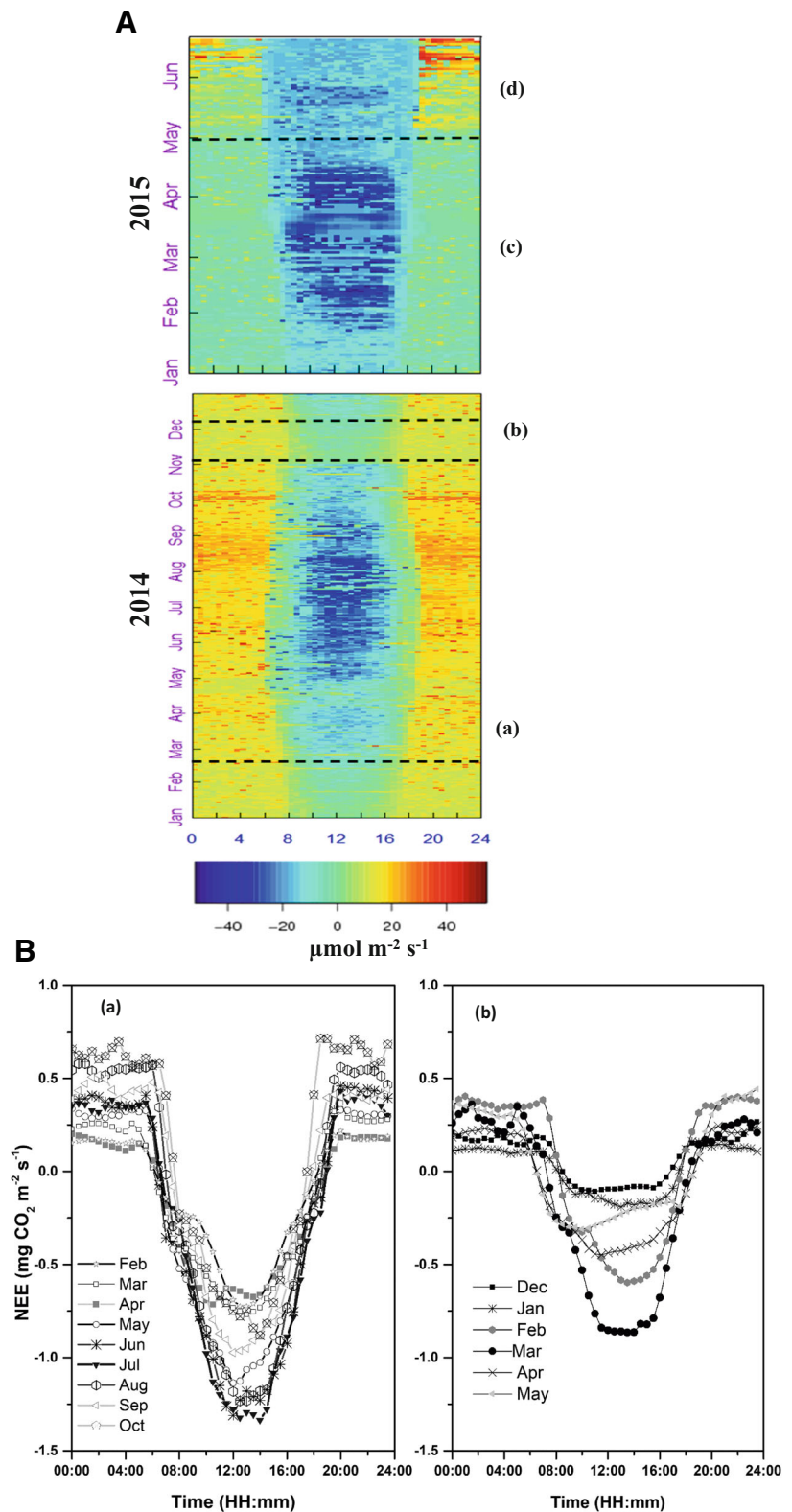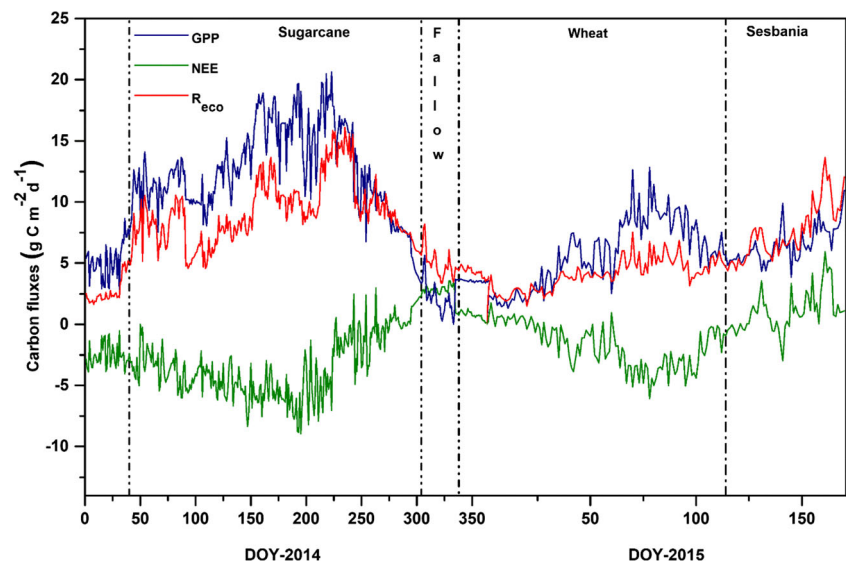

of sugarcane and wheat, there was notable diurnal variation in NEE. A distinctive U-shaped curve was observed with one absorption peak (at mid-day near noon) and two emission peaks (6:00 and 19:00 hrs). The uptake of CO_2 in the form

of negative NEE has distinct diel variation and matches with the intensity of radiation controlled by movement and position of sun in the sky. The NEE became negative with sunrise and attained peak negative value at noon hours, then after CO_2

uptake tended to decline until evening hours and NEE became positive during night hours. Later in the day, the upward peak of the curve was the result of either downward ramping of the photosynthesis, stems from a daily increase in temperature, which coincidently increases respiratory losses from soil and vegetation (Larcher, 1995) or reduction in leaf gas exchange via stomata (Goulden et al. 2004). This trend was in line with the previous findings in a range of ecosystems (Grassi et al. 2009; Wagle et al. 2015).

The diurnal peak was higher in July and March (Fig. 3) in sugarcane and wheat growing season, respectively, on account of the direct relationship of NEE with canopy closure and higher PAR values. The maximal peaks of diurnal CO_2 uptake in sugarcane and wheat crop were -2.21 mg CO_2 m^{-2} s^{-1} and -1.49 mg CO_2 m^{-2} s^{-1}, which were observed in the months of July and March, respectively. Both appeared during a maximum vegetative phase which was similar to the seasonal variation in LAI. The minimal NEE values in December 2014 and January 2015 reached up to 0.077 mg CO_2 m^{-2} s^{-1} and 0.017 mg CO_2 m^{-2} s^{-1}, depicting the weak CO_2 absorption strength after sugarcane harvesting. Similarly, NEE values in June 2015 turned positive (0.14 mg CO_2 m^{-2} s^{-1}), depicting the CO_2 source status of the study site. Higher respiration due to higher temperature and microbial activity outstripped the CO_2 uptake during that period. The daily difference of NEE in a crop field was determined by the extent of CO_2 source and sink (Jun et al., 2006). The daily difference of monthly averaged NEE was higher over the study site during the active growing period (April–August (sugarcane) and February–April (wheat)). In the sugarcane crop, it ranged from 2.04 to 3.61 mg CO_2 m^{-2} s^{-1}, while in wheat crop the range varied from 2.82 to 2.95 mg CO_2 m^{-2} s^{-1}. The higher difference in NEE during active growing season attributed to higher photosynthetic potential during the day and respiration at night.

Seasonal variation in CO_2 fluxes

In Fig. 3, the daily averaged seasonal variations of GPP, NEE, and R_{eco} are shown. Over the entire course of the study, based on positive and negative values of NEE, the ecosystem can be divided into four sections: two stages of CO_2 uptake in sugarcane and wheat growing seasons (negative NEE), one stage of CO_2 emission after sugarcane harvesting,, and another after wheat harvesting (positive NEE). Ecosystem exhibited as both carbon source and sink, depending upon the crop type and crop phenology, aligned with two major physiological activities (photosynthesis and respiration). R_{eco} was greater than GPP in early and late growing season due to low photosynthetic activity and higher respiration rates; NEE was positive, and the ecosystem was a carbon source. GPP increases with enhancement in growth stages in the sugarcane-wheat system, eventually exceeding R_{eco} due to which ecosystem acted as a carbon sink. NEE had negative periods during 32 DOY (-2.696 ± 1.212 g C m^{-2} day^{-1})–270 DOY (-1.198 ± 0.795 g C m^{-2} day^{-1}) and 60 DOY (-3.286 ± 1.848 g C m^{-2} day^{-1})–120 DOY (-1.513 ± 0.771 g C m^{-2} day^{-1}) displaying sugarcane and wheat crop canopy, respectively. Cumulative nocturnal average of CO_2 efflux during the month of October (274 DOY–282 DOY) was 37.5% higher than the CO_2 uptake, shifting NEE values clearly on the positive side tending to act as a carbon source.

Also, in December, the ecosystem maintains its carbon source characteristics as the surface was respiring due to the low vegetative growth of the wheat crop. Wheat active growing season started from the end of January (25 DOY) to mid-April (114 DOY), under which NEE values were constantly over positive side up to February depicting early growth stage in wheat crop. Crop experiences maximum CO_2 absorption after it attains canopy closure, which lasted for a shorter duration. The anthesis stage of wheat crop also possesses a limiting factor in carbon uptake rates, as the respiration exceeds

Fig. 3 Dynamics of net ecosystem CO_2 exchange (NEE), gross primary productivity (GPP), and ecosystem respiration (R_{eco}) in sugarcane-wheat-sesbania system during the 2014 and 2015 growing season. The first section displays the carbon fluxes (GPP, NEE, and R_{eco}) in sugarcane growing season while 2nd, 3rd, and 4th sections display fallow, wheat, and sesbania growing season, respectively

distinctly due to the involvement of high respiration costs in order to produce reproductive organs (Baldocchi 1994; Rochette et al. 1995). After harvesting (114 DOY), ecosystem respiration again exceeded, owing to the soil warmth and new input of fresh decomposable material, shifting the ecosystem into a carbon source. Maximal CO_2 uptake approached -8.94 g C m^{-2} day^{-1} (195 DOY) over sugarcane stand (C4) and -6.79 g C m^{-2} day^{-1} (78 DOY) over the wheat crop (C3). Differential CO_2 uptake rates in both crops were in good agreement with the results of Falge et al. (2002) and Jun et al. (2006), who reported that the maximal CO_2 uptake rates in C4 crops are higher than in C3 crop, owing to their photosynthetic pathway. Net assimilation fluxes were observed between -9 and -13 g C m^{-2} day^{-1} for the wheat crop (Anthoni et al. 2004; Béziat et al. 2009). Similar values were observed for sugar beet (Moureaux et al. 2008), rapeseed (Béziat et al. 2009), and soybean (Hollinger et al. 2005).

Just after wheat harvesting, sesbania (green manure) seeds were sown on 115 DOY, which after about 30 days, further incorporated into the soil (144 DOY), thereby increasing respiration at a higher rate. Daily average CO_2 absorption during green manuring phase reaches its maximum at -0.23 g C m^{-2} day^{-1} (141 DOY), which after higher respiration rate (due to its incorporation into the soil) continuously decreases reaching even lower than daily averaged nocturnal CO_2 efflux thus acting as a carbon source during that phase. R_{eco} was greater than GPP even during the sesbania growing season, which lowered down the carbon sequestration capacity of the ecosystem. This phenomenon could be due to the application of artificial irrigation on 132 DOY (Fig. 1) which induced favorable conditions for higher soil microbial activity thus reducing the CO_2 sequestration capacity of the ecosystem.

Cumulative carbon fluxes

The daily cumulative carbon fluxes were quantified during different crop growing seasons and illustrated in Fig. 4. The NEE, GPP, and R_{eco} were -898.24, 3696.87, and 2822.69 in the year 2014 (Fig. 4a). The values of cumulative carbon fluxes were -923.04, 3316.65, and 2433.18 g C m^{-2} during sugarcane growing season. The cumulative carbon fluxes were -123.32 (NEE), 1024.25 (GPP), and 895.83 (R_{eco}) g C m^{-2} in the year 2015 (Fig. 4b), representing wheat-sesbania (active growth phase (Ga) + Soil incorporation (Is)) growing season. When wheat and sesbania were analyzed separately, the NEE, GPP, and R_{eco} values over the wheat growing season were -192.30, 621.47, and 488.34 g C m^{-2}. Similarly, during Ga (DOY 114-DOY 144) in sesbania, cumulative NEE, GPP, and R_{eco} reached up to 7.19, 167.97, and 175.17 g C m^{-2}, respectively. The shorter growth phase in sesbania inclined the ecosystem more towards carbon source after wheat harvesting. Moreover, after Is, a considerable increase in carbon emission from the soil was found and the cumulative fluxes during that phase (DOY 144–

DOY 170) reached up to 60.49 (NEE), 347 (GPP), and 407.50 (R_{eco}) g C m^{-2}. The sudden and effective shift of the ecosystem towards a carbon source after Is may be ascertained to higher soil respiration which was further influenced by elevated temperature and addition of the labile substrate (Dash et al. 2014). Soil respiration activates carbon emission from the soil which is more strongly driven by the activities of soil microbes and plant roots. Furthermore, addition of complex organic substrates (e.g., sesbania root) deployed more C emission from the soil, ascribed to the activation of a higher number of the microbial community present in the soil (Beare et al. 1990; Hoyle and Murphy 2007).

The seasonal flux values are comparable to numerous published carbon flux values for C4 and C3 crops on a global basis, although published values are from studies conducted in areas with different local climates, soil characteristics, and management practices. Compared to recent studies in different sites (Table 1), the NEE of ratooned sugarcane in Saharanpur found less than all sites except over the ratooned sugarcane in the Sau Paulo State, Brazil (Cabral et al. 2013; Xin et al. 2020) and the first cycle of sugarcane grown in the Louisiana region of the USA (Xin et al. 2020). This could be explained by two points: (1) our study was focused on ratooned sugarcane (2nd cycle), during which lesser carbon sequestration was observed as compared to the previous growth cycle (Cabral et al. 2013); (2) shorter growth cycle of sugarcane (9 months) in India in comparison to the other sugarcane growing regions in the world (12 months).

The cumulative carbon flux value over wheat crop (C3) was higher than the results reported by Li et al. (2006), while lower than the values reported by Wang et al. (2013) and Chen et al. (2015) over wheat crop. Cumulative carbon fluxes were also lower than the values reported by Bhattacharyya et al. (2013) over rice crop in Cuttack, Orissa. Nevertheless, the maximum values of NEP and GPP were similar to the values reported by Patel et al. (2011); Bhattacharyya et al. (2013); and Wang et al. (2013) over C3 cropping system.

Comparative analysis of C3 and C4 crops

The magnitude of CO_2 flux is often related to the amount of growing plant tissue, represented by indices such as aboveground biomass and LAI (Frank and Dugas 2001; Flanagan and Johnson 2005). CO_2 fluxes were found temporally disproportionate with the leaf area index in sugarcane growing season specifically at the senescence stage, similarly as observed in corn by Baldocchi (1994). This may be due to temporal changes in canopy architecture which causes canopy assimilation rates to diverge as leaf area increases (Baldocchi 1994). Keeping the LAI and GPP values only for active phases in both growing seasons determines a strong linear relationship ($r = 0.92$). Such a linear relationship between GPP and LAI was also related in other studies (Li et al. 2005; Vitale et
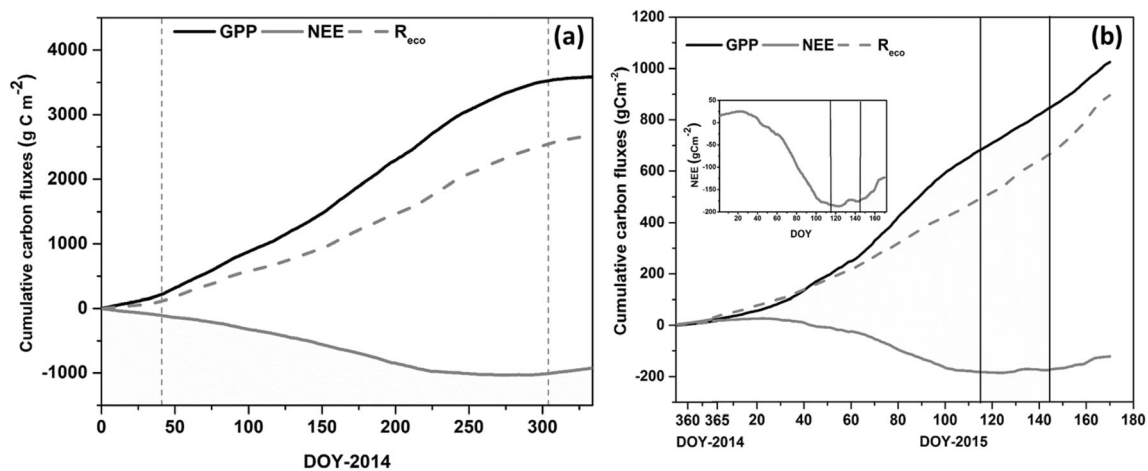
Fig. 4 Cumulative carbon fluxes in (a) sugarcane (2014), (b) wheat–sesbania (2014–2015) growing season. The dashed light gray lines in section (a) represent the start and end of the sugarcane growing season. The vertical thick lines are the harvesting period in wheat and sesbania.

The inset depicts cumulative NEE (g C m^{-2}) highlighting the variation from carbon sink to carbon source after wheat harvesting and sesbania incorporation into the soil

2016). LAI imparts a major impact on the CO_2 exchange rate of a plant canopy primarily through its control over absorption and availability of PAR for photosynthesis (Hodges and Kanemasu 1977; Hipps et al. 1983). To distinguish the impact of biological and environmental factors on canopy photosynthesis of C3 and C4 crops, we normalized GPP by LAI (Vitale et al. 2016). Further, the GPP/LAI ratio was expressed as an individual function of PAR and air temperature. The relationship between GPP/LAI and air temperature depicted the optimum temperature (T_o) for photosynthesis in C3 and C4 crops. C3 crop exhibits a T_o in the range of 12–20 °C (Fig. 5b), while C4 crop exhibits a greater photosynthetic rate at higher T_o (25–30 °C) than C3 crops. Moreover, the photosynthetic rate in C4 crop reveals narrower temperature range in comparison to C3 (Fig. 5a), as the photosynthetic rate in C4 plunged at low temperature (Yamori et al. 2014).

Similarly, GPP per unit LAI relationship with PAR reveals a steady increase in CO_2 fixation in C4 crop with an increase in light intensity in comparison to the C3 crop (Fig. 5c). This pattern elucidated more efficient use of solar energy in the case of the C4 photosynthetic pathway (Wang et al. 2012). Further to comprehend the CO_2 fixation a bit more, we selected two points of the active growth sections in both growing seasons (June (sugarcane growing season), March (wheat growing season)). CO_2 fixation in C4 crops was higher than in the C3 crop at approximately the same light intensity (C4 (250.26 μ mol m^{-2} s^{-1}), C3 (241.61 μ mol m^{-2} s^{-1})).

Response of CO_2 fluxes to environmental parameters

Daily NEE evaluation using path analysis

Path analysis was used to examine the impact of major environmental (predictor) variables on regulating NEE at daily

time step as mentioned under methodology for both sugarcane ($n = 173$) and wheat ($n = 120$) growing seasons (Fig. 6). The direct (i.e., path coefficient/DE), indirect (i.e., coupling effect/IE), and total effect (TE) of environmental variables on NEE are shown in Table S1. All the environmental variables were significantly correlated with NEE. In both growing seasons, PAR was the highly correlated variable with NEE (Table S2). PAR has the greatest DE, followed by VPD and Ta in sugarcane and wheat growing season, respectively. The direct path coefficient of PAR on NEE was −0.66 (sugarcane) and −0.74 (wheat), showing the comparatively much stronger impact of PAR on NEE during the wheat growing period.

The IE depict how the environmental variables influenced NEE through other variables under consideration. The path analysis showed that VPD (−0.410) and SWC (0.205) had stronger IE on NEE during sugarcane growing season, while Ta (−0.539) and VPD (−0.304) had stronger IE on NEE during wheat growing season. The TE of SWC (−0.205) and WAI (−0.229) on NEE was higher in sugarcane growing season, in comparison to the wheat growing season. This indicates higher dependency of sugarcane on water for growth and development (Cabral et al. 2013).

Response of day-time NEE to PAR

The relationship between day-time NEE and incident PAR was established under different VPD sections (Fig. 7). Net CO_2 uptake increases with the rise in VPD up to 20 h Pa which further started diverting in a decreasing trend with a further rise in VPD. We found R^2 between NEE and incident PAR for different VPD ranges over the whole sugarcane and wheat growing season. R^2 values were higher in VPD values ranging from 0 to 20 h Pa (0.61 (sugarcane) and 0.40 (wheat)) (95% confidence interval, $p<0.01$) in comparison to VPD ranging

Table 1 Comparative analysis of carbon fluxes of sugarcane and wheat growing season at different study sites

Site (crop)	Climate	Latitude	Season	Seasonal NEP* Cumulative (g C m⁻²)	Maximum (g C m⁻² day⁻¹)	Seasonal GPP Cumulative (g C m⁻²)	Maximum (g C m⁻² day⁻¹)	Reference
C4								
Sau Paulo State, Brazil (sugarcane)	Sub-tropical humid	21° 38' S	Cycle 1 (April 2005–May 2006) Cycle 2 (May 2006–May 2007)	1964 (±44) 960 (±64)	-	3612 2719	21 -	Cabral et al. 2013
Sau Paulo State, Brazil (sugarcane)	Sub-tropical humid	21° 63' S	Cycle 1 (May 2005–May 2006) Cycle 2 (Sep 2006–May 2007)	-	-	4035.60 2841.62	20 18	Xin et al. 2020
Sau Paulo State, Brazil (sugarcane)	Sub-tropical humid	21° 55' S	Cycle 1 (Oct 2015–Oct 2016) Cycle 2 (Oct 2016–Aug 2017) Cycle 3 (Aug 2017–Nov 2018)	2003.18 1294.63 1220.45	12.27	-	-	Cabral et al. 2020
Murwillumbah, Australia (sugarcane)	Sub-tropical humid	28° 19' S	Oct 2005–Sep 2006	1600 to 3600	-	-	-	Denmead et al. 2009
Louisiana, USA (sugarcane)	Sub-tropical humid	29° 63' N	Feb 2017–Nov 2017	-	-	2200.88	15	Xin et al. 2020
Saharanpur, India (sugarcane)	Sub-tropical dry sub-humid	29° 52' N	Cycle 2 (Feb 2014–Oct 2014)	923.04	8.94	3205	18.44	This study
C3								
Yucheng, China (wheat)	Semi-humid	30° 56' N	Oct 2002–June 2003 Oct 2003–June 2004	78 152	8.0 9.0	- -	11.98 12.03	Li et al. 2006
Changwu, China (wheat)	Humid continental	35° 14' N	Sep 2009–May 2010	218.9	≈ 5.0	512	≈ 8	Wang et al. 2013
Shouxian, China (wheat)	Semi-humid	32° 33' N	Oct 2007–May 2008 Oct 2008–May 2009 Oct 2009–May 2010	583 512 451	10.9 to 11	1220 1135 859	-	Chen et al. 2015
CRRI, Cuttack, India (rice)	Sub-tropical monsoon	20° 27' N	July–November 2012	448	6	811	≈ 11	Bhattarcharya et al. 2014
Meerut, India	Sub-tropical humid	29° 05' N	Dec 2009–April 2009	-	6.5	-	13.47	Patel et al. 2011
Saharanpur, India (wheat)	Sub-tropical dry sub-humid	29° 52' N	Dec 2014–April 2015	192.30	6.79	621.47	13.32	This study

*For convenience, the sign convention has changed. NEP (net primary productivity) is equal to −NEE
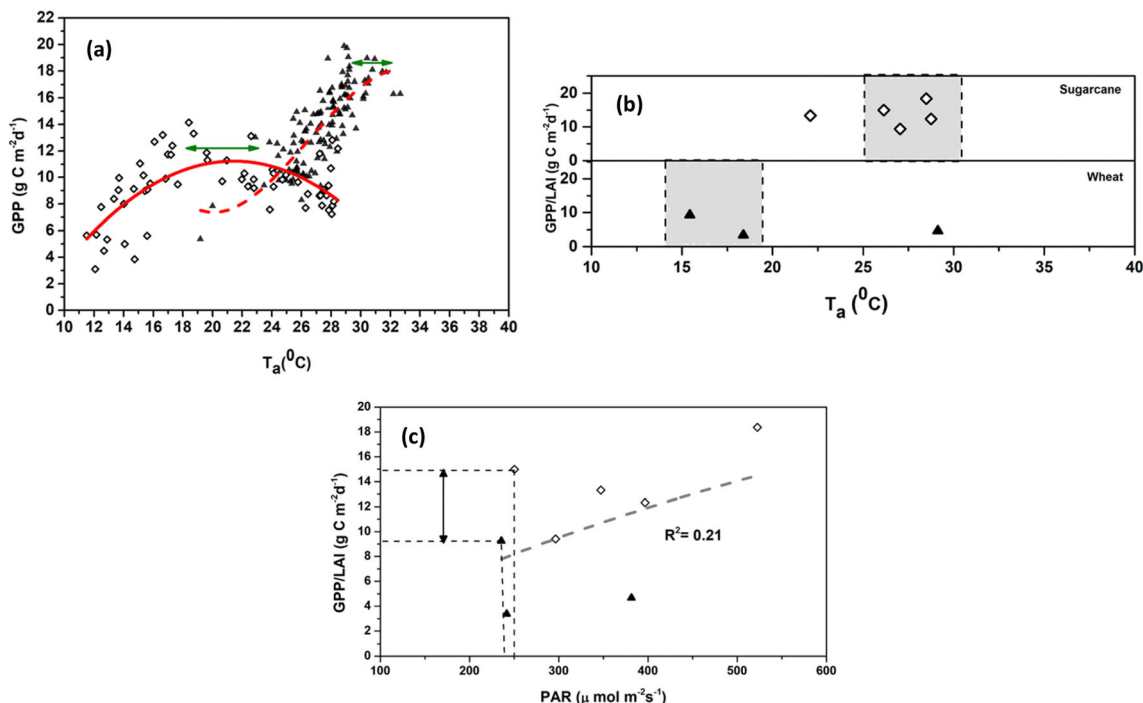
Fig. 5 (a) The relationship between GPP and air temperature in sugarcane (C4) and wheat growing seasons, and (b) and (c) depict response of GPP per unit of LAI (GPP/LAI) to air temperature (°C) and photosynthetic active radiation (μ mol m^{-2} s^{-1}), respectively

from 20 to 40 h Pa (0.41 (sugarcane) and 0.25 (wheat)) (95% confidence interval, $p<0.01$). The net CO_2 uptake reached up to −2.0 mg CO_2 m^{-2} s^{-1} and −1.45 mg CO_2 m^{-2} s^{-1} when VPD ranges from 0 to 20 hPa in sugarcane and wheat growing season, respectively. On the contrary, the net CO_2 uptake decreases and reached up to −1.6 mg CO_2 m^{-2} s^{-1} and −1.0 mg CO_2 m^{-2} s^{-1} when VPD ranges from 20 to 40 hPa in sugarcane and wheat growing season, respectively.

The decrease in net CO_2 uptake beyond 20 hPa was may be due to the effect of higher VPD on stomatal conductance. Decrease in stomatal conductance further influences

carboxylation rate as vegetation absorbs CO_2 from the atmosphere through stomata.

Response of night-time NEE (Rn) to air temperature

Respiration comprises of both autotrophic and heterotrophic respiration, which are predominantly controlled by temperature and soil moisture (Flanagan and Johnson 2005; Nakano et al. 2008). Therefore, we plotted the Rn against the air temperature in both sugarcane (Fig. 8a) and wheat growing seasons (Fig. 8b), under varying soil water conditions measured
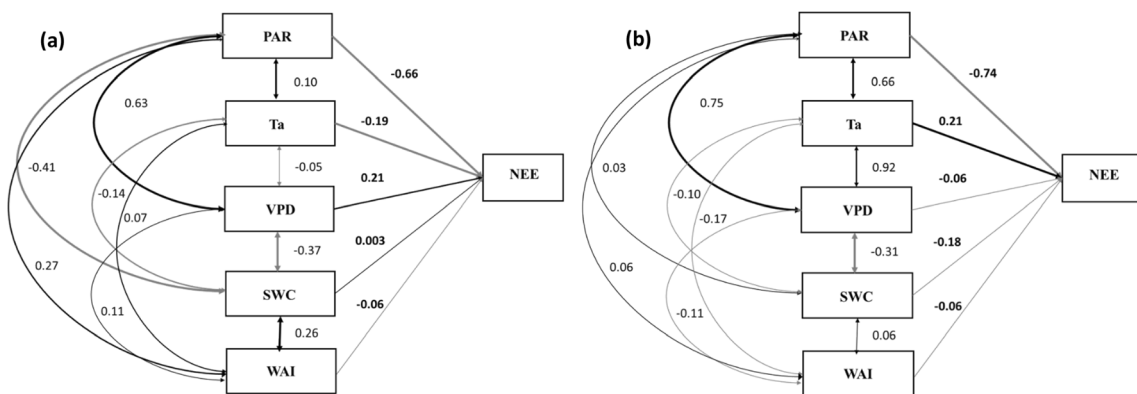
Fig. 6 Path diagrams illustrating effect of photosynthetic active radiation (PAR), air temperature (Ta), vapor pressure deficit (VPD), soil water content (SWC), and water availability index (WAI) on daily net ecosystem exchange (NEE) during (a) sugarcane growing season ($n = 173$) and (b) wheat growing season ($n = 120$). Analysis was based on daily average

of all variables considered. Black arrows represent positive paths; gray arrows represent negative paths. Bold numbers indicate standard path coefficient. Arrow width indicates the significant correlation at $p<0.05$ between the environmental variables

Fig. 7 Relationship between NEE and PAR in (a) sugarcane growing season and (b) wheat growing season at 0<VPD<20 hPa and 20 hPa< VPD<40 hPa. Dark gray colored closed up triangles represent the net CO_2 uptake at VPD range from 0 to 20 hPa, while light gray colored open circles represent the net CO_2 uptake at VPD range from 20 to 40 hPa
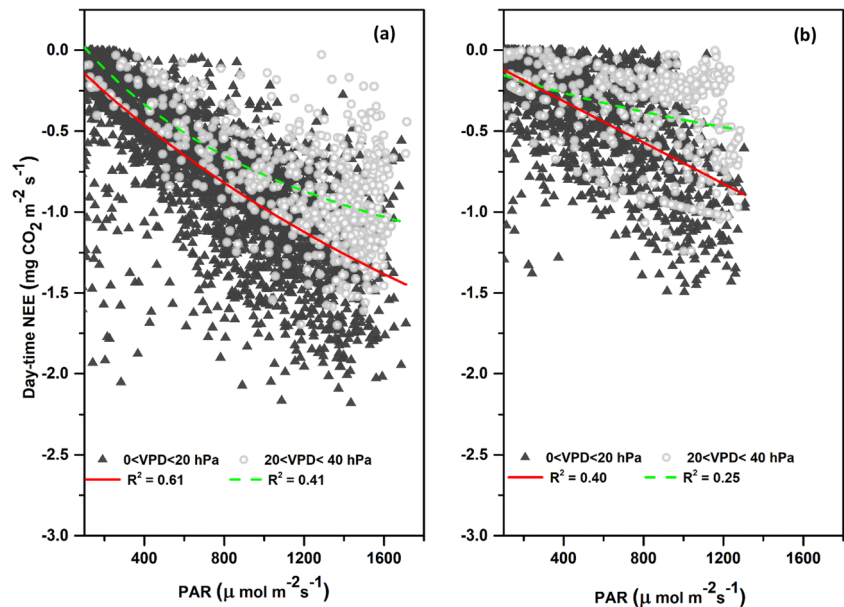
at a depth of 7.5 cm (SWC). As expected, Rn during sugarcane growing season was significantly larger than during wheat growing season which reflects greater plant respiration of sugarcane owing to its greater biomass (Nakano et al. 2008)

In our study, Rn was exponentially related to the corresponding temperature. An exponential relationship between night-time respiration and air temperature has been previously described (Suyker et al. 2004; Wang et al. 2013; Vote et al. 2015; Chen et al. 2015). Optimum soil moisture ($0.33 \leq SWC < 0.42$ m^{-3} (sugarcane) and $0.31 \leq SWC < 0.37$ m^3 m^{-3} (wheat)) leads to higher correlation between NEE and air temperature. Further, the correlation values were arranged under

different soil moisture conditions as water sufficient condition> water deficit condition> water excess conditions ranging from 0.64 to 0.87 (95% confidence interval, $p<0.0001$) and 0.38 to 0.75 (95% confidence interval, $p<0.0001$) over sugarcane and wheat growing season, respectively.

Q_{10} was calculated from Eq. 3, which varied from 1.12 to 2.18 (2.03–2.18 (sugarcane), 1.12–1.54 (wheat)) influenced by environmental temperature, substrate availability, and soil moisture (Davidson et al., 2006; Nakano et al. 2008; Jingxue et al., 2019). Contrary to the previous studies reported (Nakano et al. 2008; Jingxue et al., 2019), Q_{10} was higher under water sufficient condition in both growing seasons.

Fig. 8 Response of night-time respiration (R_{eco}) to air temperature (Ta) over (a) sugarcane growing season and (b) wheat growing season under water sufficient conditions (open black circle), water deficit condition (open black square), and water excess condition (closed grayish triangle). Date was bin averaged at 1 °C
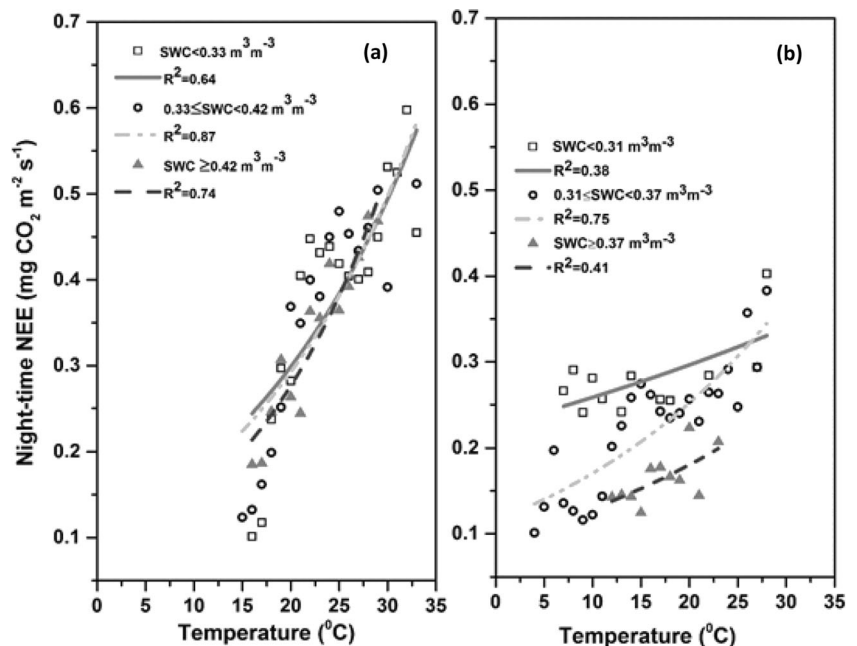
Lower Q_{10} values under water deficit and water excess conditions could be the impact of suppressed respiration activity under both the conditions.

Comparison of GPP product against observed GPP

The available satellite GPP products (GPP$_{MOD}$ and GPP$_{VPM}$) were compared against the GPP$_{EC}$ (Fig. 9). The GPP$_{MOD}$ (R^2 = 0.02, RMSE = 8.74 g C m^{-2} day^{-1}) has showed very low performance in comparison to the GPP$_{VPM}$ (R^2 = 0.63, RMSE = 4.63 g C m^{-2} day^{-1}). Various studies also depicted the poor results of GPP$_{MOD}$ over the agricultural sites (Zhang et al. 2012; Wang et al. 2017). The poor performance of GPP$_{MOD}$ can be attributed to its two major assumptions: (1) constant LUE value for individual biome type; (2) APAR (PAR × fPAR) is the energy absorbed by the entire canopy (Zhang et al. 2017). The GPP$_{MOD}$ is primarily based on the leaf quantity (amount of the leaf area). Though recent studies have depicted that not only leaf quantity but also leaf quality (photosynthetic rate of the individual leaf) is also a major determinant of the photosynthetic capacity (Wu et al. 2016). The leaf quality is based on the leaf chlorophyll content and it is not only dependent upon the environment and nutrient availability but also regulated by the phenology. Further, the phenological variations regulate the seasonal GPP variations. Unlike GPP$_{MOD}$, GPP$_{VPM}$ take leaf quality into consideration in the form of fraction of PAR absorbed by chlorophyll (fPARchl), which is computed from the EVI. It can better capture the seasonal variation in the photosynthetic capacity and can further improve the seasonal representation of the GPP (Zhang et al. 2009, 2014).

The 8-day variation in the GPP$_{VPM}$ and GPP$_{EC}$ from January 2014 to June 15 is depicted through Fig. 9a and Fig. S2. The result showed that the GPP$_{VPM}$ has

moderately captured the seasonal variation in GPP$_{EC}$ over sugarcane-wheat-based system. Considering GPP$_{EC}$ as the reference, the GPP$_{VPM}$ and GPP$_{MOD}$ underestimated the GPP by 36% and 66%, respectively. Similar results have been observed by Xin et al. (2020) over the sugarcane crop in Louisiana, USA. We also assessed the biophysical variation of EVI in terms of GPP dynamics (Fig. 9b). The relationship between EVI and GPP$_{EC}$ (R^2 = 0.49) was also established to address the moderate results from the comparative analysis of GPP$_{EC}$ and GPP$_{VPM}$. The EVI showed the seasonal phenological variations during the whole growing season, but performed moderately to capture the peak growing period (Fig. 10B). This could be due to the shorter footprint (250–300 m) of the EC site and heterogeneity of the land surface. The GPP products are available at 500 m resolution, which takes into account a large footprint area around EC site with higher heterogeneity which ultimately lead to the consideration of the mixed pixels.

To the best of our knowledge, the comparative study of satellite-based GPP products and GPP$_{EC}$ was never done in India particularly over the sugarcane (C4)-wheat (C3)-based system, though various comparative studies have been well evaluated over the croplands in India which only include the crops with the C3 photosynthetic pathway (Patel et al. 2011). The continuous evaluation of the GPP$_{EC}$ and satellite-based GPP over different ecosystems and over the vegetation with different photosynthetic pathways is imperative to accurately upscale the GPP at regional or global scale. Owing to the continuous and systematic measurements over different vegetation and ecosystems, satellite remote sensing plays an important role for global GPP quantification. Further, the GPP estimation at regional, continent, or at global scale can improve our understanding of the feedbacks between the atmosphere and the terrestrial biosphere in context of the climate
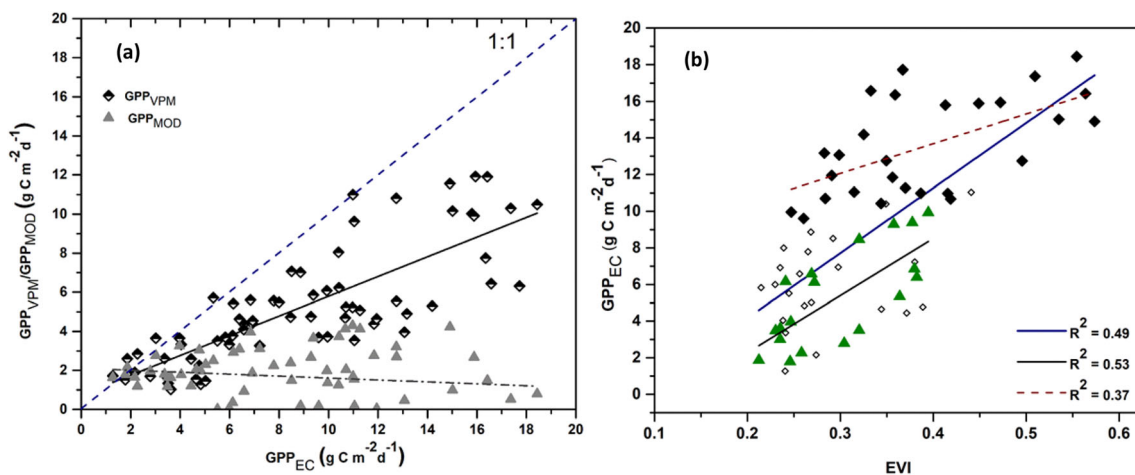
Fig. 9 Relationship of (a) satellite-based GPP products (GPP$_{VPM}$ and GPP$_{MOD}$) and (b) MODIS-based EVI against GPP$_{EC}$. The half-filled diamonds represent the relationship between GPP$_{EC}$ and GPP$_{VPM}$ while the dark gray colored stars represent the relationship between GPP$_{EC}$ and GPP$_{MOD}$. Solid black diamond, solid green up triangles, and open diamond represent the EVI vs GPP during sugarcane growing season, wheat growing season, and whole study period, respectively

change and further can facilitate climate-policy making (Canadell et al. 2007; Xiao et al. 2008).

Conclusions

In order to understand the dynamics of CO_2 fluxes (NEE, R_{eco}, and GPP) over C4-C3 crops in sub-tropical dry sub-humid climate, the seasonal variation of carbon fluxes and the controlling environmental variables over sugarcane-wheat-sesbania-based system was analyzed from 2014 to 2015 using the EC measurements and the ancillary environmental variables.

Results indicated that sugarcane being a C4 (high biomass crop) engaged in more carbon sequestration in comparison to wheat. The diurnal dynamics of NEE over the ecosystem depicted the carbon sink capability in sugarcane from May to August whereas wheat exhibits a peak of carbon sequestration by the end of March in the year 2015. Just after wheat harvest, the ecosystem becomes a carbon source up to sesbania sowing, which further acted as a carbon source owing to the increase in respiration activity due to the incorporation of sesbania into the soil (144 DOY). The cumulative NEE was -923.04 g C m^{-2} and -192.30 g C m^{-2} for sugarcane and wheat growing season, respectively. CO_2 fluxes were jointly affected by multiple environmental parameters. Path analysis indicated that PAR was the most important predictor variable affecting daily NEE over both growing seasons. The variation of GPP_{EC} with the satellite products was also evaluated. This is the first case study in India to evaluate the flux dynamics over C4-C3 cropping system. Furthermore, the present study evaluates the broad aspects ranging from micrometeorology to remote sensing. The results are also important for accurate modelling of agroecosystem for this area and further planning for the effects of climate change.

Author contribution Designed research; NRP, PC, VK, and NRP collected data as well as performed research; SP and NRP analyzed data and drafted a manuscript with inputs from PC; critical suggestions and review of manuscript by PC and VK.

Declarations

Conflict of Interest The authors declare no conflict of interest

References

Allen RG, Pereira LS, Raes D, et al (1998) Crop evapotranspiration-guidelines for computing crop water requirements. Irrig Drain Pap No 56, FAO 300

Anderson RG, Tirado-Corbalá R, Wang D, Ayars JE (2015) Long-rotation sugarcane in Hawaii sustains high carbon accumulation and radiation use efficiency in 2nd year of growth. Agric Ecosyst Environ 199:216–224. https://doi.org/10.1016/j.agee.2014.09.012

Ansley RJ, Dugas WA, Heuer ML, Kramp BA (2002) Bowen ratio/energy balance and scaled leaf measurements of CO2 flux over burned Prosopis savanna. Ecol Appl 12:948. https://doi.org/10.2307/3061029

Anthoni PM, Knohl A, Rebmann C, Freibauer A, Mund M, Ziegler W, Kolle O, Schulze ED (2004) Forest and agricultural land-use-dependent CO2 exchange in Thuringia, Germany. Glob Chang Biol 10:2005–2019. https://doi.org/10.1111/j.1365-2486.2004.00863.x

Aubinet M, Grelle A, Ibrom A et al (1999) Estimates of the annual net carbon and water exchange of forests: the EUROFLUX methodology. Adv Ecol Res 30:113–175. https://doi.org/10.1016/S0065-2504(08)60018-5

Aubinet M, Moureaux C, Bodson B, Dufranne D, Heinesch B, Suleau M, Vancutsem F, Vilret A (2009) Carbon sequestration by a crop over a 4-year sugar beet/winter wheat/seed potato/winter wheat rotation cycle. Agric For Meteorol 149:407–418. https://doi.org/10.1016/j.agrformet.2008.09.003

Baldocchi D (1994) A comparative study of mass and energy exchange rates over a closed C3 (wheat) and an open C4 (corn) crop: II. CO2 exchange and water use efficiency. Agric For Meteorol 67:291–321. https://doi.org/10.1016/0168-1923(94)90008-6

Baldocchi D, Falge E, Wilson K (2001) A spectral analysis of biosphere-atmosphere trace gas flux densities and meteorological variables across hour to multi-year time scales. Agric For Meteorol 107:1–27. https://doi.org/10.1016/S0168-1923(00)00228-8

Bassow SL, Bazzaz FA (1998) How environmental conditions affect canopy leaf-level photosynthesis in four deciduous tree species. Ecology 79:2660. https://doi.org/10.2307/176508

Beare MH, Neely CL, Coleman DCHW (1990) A substrate-induced respiration (SIR) method for measurement of fungal and bacterial biomass on plant residues. Soil Biol Biochem 22:585–594

Béziat P, Ceschia E, Dedieu G (2009) Carbon balance of a three crop succession over two cropland sites in South West France. Agric For Meteorol 149:1628–1645. https://doi.org/10.1016/j.agrformet.2009.05.004

Bhattacharyya P, Neogi S, Roy KS, Dash PK, Tripathi R, Rao KS (2013) Net ecosystem CO2 exchange and carbon cycling in tropical lowland flooded rice ecosystem. Nutr Cycl Agroecosyst 95:133–144. https://doi.org/10.1007/s10705-013-9553-1

Cabral OMR, Rocha HR, Gash JH, Ligo MAV, Ramos NP, Packer AP, Batista ER (2013) Fluxes of CO2 above a sugarcane plantation in Brazil. Agric For Meteorol 182–183:54–66. https://doi.org/10.1016/j.agrformet.2013.08.004

Canadell JG, Le Qué RC, Raupach MR et al (2007) Contributions to accelerating atmospheric CO2 growth from economic activity, carbon intensity, and efficiency of natural sinks. Proc Natl Acad Sci 104:18866–18870

Ceschia E, Béziat P, Dejoux J-F, Aubinet M, Bernhofer C, Bodson B, Buchmann N, Carrara A, Cellier P, di Tommasi P, Elbers JA, Eugster W, Grünwald T, Jacobs CMJ, Jans WWP, Jones M, Kutsch W, Lanigan G, Magliulo E, Marloie O, Moors EJ, Moureaux C, Olioso A, Osborne B, Sanz MJ, Saunders M, Smith P, Soegaard H, Wattenbach M (2010) Management effects on net ecosystem carbon and GHG budgets at European crop sites. Agriculture, Ecosystems and Environ-ment, Elsevier Masson

Agriculture, Ecosystems and Envi. Ecosyst Environ 139:363–383. https://doi.org/10.1016/j.agee.2010.09.020ï

Chatterjee A, Roy A, Chakraborty S, Karipot AK, Sarkar C, Singh S, Ghosh SK, Mitra A, Raha S (2018) Biosphere atmosphere exchange of CO2, H2O vapour and energy during spring over a high altitude Himalayan forest in eastern India. Aerosol Air Qual Res 18:2704–2719. https://doi.org/10.4209/aaqr.2017.12.0605

Chen C, Li D, Zhiqiu G et al (2015) Seasonal and interannual variations of carbon exchange over a rice-wheat rotation system on the North China Plain. Adv Atmos Sci 32:1365–1380. https://doi.org/10.1007/s00376-015-4253-1

Chi J, Maureira F, Waldo S, Pressley SN, Stöckle CO, O'Keeffe PT, Pan WL, Brooks ES, Huggins DR, Lamb BK (2017) Carbon and water budgets in multiple wheat-based cropping systems in the inland Pacific Northwest US: comparison of CropSyst simulations with eddy covariance measurements. Front Ecol Evol 5. https://doi.org/10.3389/fevo.2017.00050

Dash PK, Roy KS, Neogi S, Nayak AK, Bhattacharyya P (2014) Gaseous carbon emission in relation to soil carbon fractions and microbial diversities as affected by organic amendments in tropical rice soil. Arch Agron Soil Sci 60:1345–1361. https://doi.org/10.1080/03650340.2014.888714

Davis SC, Parton WJ, Del Grosso SJ et al (2012) Impact of second-generation biofuel agriculture on greenhouse-gas emissions in the corn-growing regions of the US. Front Ecol Environ 10:69–74. https://doi.org/10.1890/110003

de Vries SC, van de Ven G, van Ittersum M (2010) Resource use efficiency and environmental performance of nine major biofuel crops, processed by first-generation conversion techniques. Biomass Bioenergy 34:588–601

Deb Burman PK, Sarma D, Morrison R, Karipot A, Chakraborty S (2019) Seasonal variation of evapotranspiration and its effect on the surface energy budget closure at a tropical forest over north-east India. J Earth Syst Sci 128. https://doi.org/10.1007/s12040-019-1158-x

Deb Burman PK, Shurpali NJ, Chowdhuri S et al (2020) Eddy covariance measurements of CO2 exchange from agro-ecosystems located in subtropical (India) and boreal (Finland) climatic conditions. J Earth Syst Sci 129. https://doi.org/10.1007/s12040-019-1305-4

Denmead OT, MacDonald BCT, White I, Griffith DWT, Bryant G, Naylor T, Wilson SR (2009) Evaporation and carbon dioxide exchange by sugarcane crops. Proc Aust Soc Sugar Cane Technol 31:116–124

Falge E, Tenhunen Pflanzenökologie J, Baldocchi DD, et al (2002) Phase and amplitude of ecosystem carbon release and uptake potentials as derived from FLUXNET measurements. Part of the Natural Resources and Conserv

Flanagan LB, Johnson BG (2005) Interacting effects of temperature, soil moisture and plant biomass production on ecosystem respiration in a northern temperate grassland. Agric For Meteorol 130:237–253. https://doi.org/10.1016/j.agrformet.2005.04.002

Frank AB, Dugas WA (2001) Carbon dioxide fluxes over a northern, semiarid, mixed-grass prairie. Agric For Meteorol 108:317–326. https://doi.org/10.1016/S0168-1923(01)00238-6

Glenn AJ, Amiro BD, Tenuta M, Stewart SE, Wagner-Riddle C (2010) Carbon dioxide exchange in a northern Prairie cropping system over three years. Agric For Meteorol 150:908–918. https://doi.org/10.1016/j.agrformet.2010.02.010

Goldemberg J, Coelho S, Policy PG-E (2008) U (2008) The sustainability of ethanol production from sugarcane. Energy Policy 36:2086–2097

Goulden ML, Miller SD, Da Rocha HR et al (2004) Diel and seasonal patterns of tropical forest CO2 exchange. Ecol Appl 14:42–54. https://doi.org/10.1890/02-6008

Grassi G, Ripullone F, Borghetti M, Raddi S, Magnani F (2009) Contribution of diffusional and non-diffusional limitations to mid-day depression of photosynthesis in Arbutus unedo L. Trees - Struct Funct 23:1149–1161. https://doi.org/10.1007/s00468-009-0355-7

Hernandez-Ramirez G, Hatfield JL, Parkin TB, et al (2011) Carbon dioxide fluxes in corn-soybean rotation in the midwestern U.S.: inter- and intra-annual variations, and biophysical controls. Elsevier. https://doi.org/10.1016/j.agrformet.2011.07.017

Hipps LE, Asrar G, Kanemasu ET (1983) Assessing the interception of photosynthetically active radiation in winter wheat. Agric Meteorol 28:253–259. https://doi.org/10.1016/0002-1571(83)90030-4

Hodges T, Kanemasu ET (1977) Modeling daily dry matter production of winter wheat 1. Agron J 69:974–978. https://doi.org/10.2134/agronj1977.00021962006900060018×

Hollinger S, Bernacchi C, Forest TM-A and, 2005 U (2005) Carbon budget of mature no-till ecosystem in North Central Region of the United States. Agric For Meteorol 130:59–69

Hoyle FC, Murphy DV (2007) Microbial response to the addition of glucose in low-fertility soils SoilsWest View project. Artic Biol Fertil Soils 44:571–579. https://doi.org/10.1007/s00374-007-0237-3

Huxman TE, Sparks J, Harley P (2003) Temperature as a control over ecosystem CO2 fluxes in a high-elevation, subalpine forest Woody legume encroachment effects on dryland nitrogen cycling View project. Springer 134:537–546. https://doi.org/10.1007/s00442-002-1131-1

Jha C, Chand TK, Suraj R, et al (2013) Establishment of Eddy-Flux Network in India for NEE Monitoring

Kaul M, Dadhwal VK, Mohren GMJ (2009) Land use change and net C flux in Indian forests. For Ecol Manag 258:100–108. https://doi.org/10.1016/j.foreco.2009.03.049

Kim J, Verma SB, Clement RJ (1992) Carbon dioxide budget in a temperate grassland ecosystem. J Geophys Res 97:6057–6063. https://doi.org/10.1029/92jd00186

Lei H, Yang D, Shen Y, Liu Y, Zhang Y (2011) Simulation of evapotranspiration and carbon dioxide flux in the wheat-maize rotation croplands of the North China Plain using the Simple Biosphere Model. Hydrol Process 25:3107–3120. https://doi.org/10.1002/hyp.8026

Li C (1981) Path analysis-a primer.

Li S-G, Asanuma J, Eugster W, Kotani A, Liu JJ, Urano T, Oikawa T, Davaa G, Oyunbaatar D, Sugita M (2005) Net ecosystem carbon dioxide exchange over grazed steppe in central Mongolia. Glob Chang Biol 11:1941–1955. https://doi.org/10.1111/j.1365-2486.2005.01047.x

Li J, Yu Q, Sun X, Tong X, Ren C, Wang J, Liu E, Zhu Z, Yu G (2006) Carbon dioxide exchange and the mechanism of environmental control in a farmland ecosystem in North China Plain. Sci China Ser D Earth Sci 49:226–240. https://doi.org/10.1007/s11430-006-8226-1

Mielnick PC, Dugas WA (2000) Soil CO2 flux in a tallgrass prairie. Soil Biol Biochem 32:221–228

Moureaux C, Debacq A, Hoyaux J et al (2008) Carbon balance assessment of a Belgian winter wheat crop (Triticum aestivum L.). Glob Chang Biol 14:1353–1366. https://doi.org/10.1111/j.1365-2486.2008.01560.x

Murayama S, Saigusa N, Chan D, Yamamoto S, Kondo H, Eguchi Y (2003) Temporal variations of atmospheric CO2 concentration in a temperate deciduous forest in central Japan. Taylor Fr 55:232–243. https://doi.org/10.3402/tellusb.v55i2.16751

Nakano T, Nemoto M, Shinoda M (2008) Environmental controls on photosynthetic production and ecosystem respiration in semi-arid grasslands of Mongolia. Agric For Meteorol 148:1456–1466. https://doi.org/10.1016/j.agrformet.2008.04.011

Patel NR, Dadhwal VK, Saha SK (2011) Measurement and scaling of carbon dioxide (CO2) exchanges in wheat using flux-tower and remote sensing. J Indian Soc Remote Sens 39:383–391. https://doi.org/10.1007/s12524-011-0107-1

Pathak PS, Dagar JC, Kaushal R, Chaturvedi OP (2014) Agroforestry inroads from the traditional two-crop systems in heartlands of the

Indo-Gangetic Plains. In: Agroforestry Systems in India: Livelihood Security & Ecosystem Services,. pp 87–116

Patra PK, Canadell JG, Houghton RA, Piao SL, Oh NH, Ciais P, Manjunath KR, Chhabra A, Wang T, Bhattacharya T, Bousquet P, Hartman J, Ito A, Mayorga E, Niwa Y, Raymond PA, Sarma VVSS, Lasco R (2013) The carbon budget of South Asia. Biogeosciences 10:513–527. https://doi.org/10.5194/bg-10-513-2013

Pearcy RW, Ehleringer J (1984) Comparative ecophysiology of C3 and C4 plants. Plant Cell Environ 7:1–13. https://doi.org/10.1111/j.1365-3040.1984.tb01194.x

Rochette P, Desjardins RL, Pattey E, Lessard R (1995) Crop net carbon dioxide exchange rate and radiation use efficiency in soybean. Agron J 87:22–28. https://doi.org/10.2134/agronj1995.00021962008700010005×

Saha S, Chakraborty D, Sehgal V et al (2015) Potential impact of rising atmospheric CO_2 on quality of grains in chickpea (Cicer arietinum L.). Food Chem 187:431–436

Saito M, Kato T, Tang Y (2009) Temperature controls ecosystem CO_2 exchange of an alpine meadow on the northeastern Tibetan Plateau. Glob Chang Biol 15:221–228. https://doi.org/10.1111/j.1365-2486.2008.01713.x

Sarma D, Kumar Baruah K, Baruah R et al (2018) Carbon dioxide, water vapour and energy fluxes over a semi-evergreen forest in Assam, Northeast India. J Earth Syst Sci 127:94. https://doi.org/10.1007/s12040-018-0993-5

Soegaard H, Jensen NO, Boegh E, et al (2003) Carbon dioxide exchange over agricultural landscape using eddy correlation and footprint modelling

Suyker AE, Verma SB, Burba GG, Arkebauer TJ, Walters DT, Hubbard KG (2004) Growing season carbon dioxide exchange in irrigated and rainfed maize. Agric For Meteorol 124:1–13. https://doi.org/10.1016/j.agrformet.2004.01.011

Teixeira L, Corradi M, Fukuda A et al (2013) Soil and crop residue CO2-C emission under tillage systems in sugarcane-producing areas of southern Brazil. Sci Agric 70:327–335

Vitale L, Di Tommasi P, D'Urso G, Magliulo V (2016) The response of ecosystem carbon fluxes to LAI and environmental drivers in a maize crop grown in two contrasting seasons. Int J Biometeorol 60:411–420. https://doi.org/10.1007/s00484-015-1038-2

Vote C, Hall A, Charlton P (2015) Carbon dioxide, water and energy fluxes of irrigated broad-acre crops in an Australian semi-arid climate zone. researchoutput.csu.edu.au 73:449–465. https://doi.org/10.1007/s12665-014-3547-4

Waclawovsky AJ, Sato PM, Lembke CG, Moore PH, Souza GM (2010) Sugarcane for bioenergy production: an assessment of yield and regulation of sucrose content. Plant Biotechnol J 8:263–276

Wagle P, Xiao X, Suyker AE (2015) Estimation and analysis of gross primary production of soybean under various management practices and drought conditions. ISPRS J Photogramm Remote Sens 99:70–83. https://doi.org/10.1016/j.isprsjprs.2014.10.009

Wang H, Li Xin TJ (2020) Interannual variations of evapotranspiration and water use efficency over an oasis cropland in arid regions of North-Western China. Water 12

Wang C, Guo L, Li Y, Wang Z (2012) Systematic comparison of C3 and C4 plants based on metabolic network analysis. BMC Syst Biol 6. https://doi.org/10.1186/1752-0509-6-S2-S9

Wang W, Liao Y, Wen X et al (2013) Dynamics of CO2 fluxes and environmental responses in the rain-fed winter wheat ecosystem of the Loess Plateau, China. Sci Total Environ 461:10–18

Wang L, Zhu H, Lin A, Zou L, Qin W, du Q (2017) Evaluation of the latest MODIS GPP products across multiple biomes using global eddy covariance flux data. Remote Sens 9:418. https://doi.org/10.3390/rs9050418

Watham T, Kushwaha SPS, Patel NR, Dadhwal VK (2014) Monitoring of carbon dioxide and water vapour exchange over a young mixed forest plantation using eddy covariance technique

Wu J, Albert LP, Lopes AP et al (2016) Leaf development and demography explain photosynthetic seasonality in Amazon evergreen forests. Science 351(80):972–976. https://doi.org/10.1126/science.aad5068

Xiao J, Zhuang Q, Baldocchi D et al (2008) Estimation of net ecosystem carbon exchange for the conterminous United States by combining MODIS and AmeriFlux data. Agric For Meteorol 148:1827–1847

Xin F, Xiao X, Cabral OMR, White PM Jr, Guo H, Ma J, Li B, Zhao B (2020) Understanding the land surface phenology and gross primary production of sugarcane plantations by eddy flux measurements, MODIS images, and data-driven models. Remote Sens 12:2186. https://doi.org/10.3390/rs12142186

Xu M, Qi Y (2001) Spatial and seasonal variations of Q10 determined by soil respiration measurements at a Sierra Nevadan forest. Glob Biogeochem Cycles 15:687–696. https://doi.org/10.1029/2000GB001365

Yamori W, Hikosaka K, Way DA et al (2014) Temperature response of photosynthesis in C 3, C 4, and CAM plants: temperature acclimation and temperature adaptation. Photosynth Res 119:101–117. https://doi.org/10.1007/s11120-013-9874-6

Yongqiang Z, Yanjun S, Qiang Y, Changming L, Kondoh A, Changyuan T, Hongyong S, Jinsheng J (2002) Variation of fluxes of water vapor, sensible heat and carbon dioxide above winter wheat and maize canopies. J Geogr Sci 12:295–300. https://doi.org/10.1007/bf02837548

Zhang Q, Middleton EM, Margolis HA, Drolet GG, Barr AA, Black TA (2009) Can a satellite-derived estimate of the fraction of PAR absorbed by chlorophyll (FAPARchl) improve predictions of light-use efficiency and ecosystem photosynthesis for a boreal aspen forest? Remote Sens Environ 113:880–888. https://doi.org/10.1016/j.rse.2009.01.002

Zhang F, Chen JM, Chen J, Gough CM, Martin TA, Dragoni D (2012) Evaluating spatial and temporal patterns of MODIS GPP over the conterminous U.S. against flux measurements and a process model. Remote Sens Environ 124:717–729. https://doi.org/10.1016/j.rse.2012.06.023

Zhang Q, Ben CY, Lyapustin AI et al (2014) Estimation of crop gross primary production (GPP): fAPARchl versus MOD15A2 FPAR. Remote Sens Environ 153:1–6. https://doi.org/10.1016/j.rse.2014.07.012

Zhuang Q, Melillo JM, Kicklighter DW, Prinn RG, McGuire AD, Steudler PA, Felzer BS, Hu S (2004) Methane fluxes between terrestrial ecosystems and the atmosphere at northern high latitudes during the past century: a retrospective analysis with a process-based biogeochemistry model. Glob Biogeochem Cycles 18. https://doi.org/10.1029/2004GB002239